the calculation of the scattering phase shifts. This observation parallels the well-known fact in bound-state shell-model calculations that energy levels are less sensitive to the model wave functions than transition rates. A fairly good description of the scattering process is probably obtained even with rather crude approximations. The energy dependence of the total wave function of the system appears to be quite important in explaining the shape of the photoabsorption cross section.

3. Not too much can be said concerning the energy dependence (or nonlocality) of the shell-model potential. However, we feel that at least part of the discrepancy may be removed by a more refined choice of the shell-model potential or the effective interaction.

Note added in proof. Recently another calculation of the photodisintegration cross section of He^4 has appeared [F. Beck and A. Müller Aruke, Phys. Letters **27B**, 343 (1968)].

ACKNOWLEDGMENT

One of the authors (J.H.) would like to thank Professor Feshbach for the hospitality extended to him at the Center for Theoretical Physics.

PHYSICAL REVIEW VOLUME 175, NUMBER 4 20 NOVEMBER 1968

π^--^{4}He Inelastic and Capture Reactions Leading to Excited and Multineutron Final States

LEON KAUFMAN, VICTOR PEREZ-MENDEZ, AND JOHN SPERINDE
Lawrence Radiation Laboratory, University of California, Berkeley, California 94720
(Received 17 May 1968)

A beam of (140±0.5)-MeV π^- was produced at the Berkely 184-in. cyclotron and used to study the final-state interactions of three and four neutrons, and to look for excited levels of the α particle through the reactions

$$\begin{aligned}\pi^-+{}^4\mathrm{He} &\rightarrow \pi^-+{}^4\mathrm{He}^*,\\ &\rightarrow p+3n,\\ &\rightarrow d+2n,\\ &\rightarrow \pi^++4n.\end{aligned}$$

Only one such level is found, with an excitation energy of 32 MeV and an intrinsic width smaller than our 1-MeV resolution. We find that our data on the four-neutron final state, although not inconsistent with phase space, agree more closely with the assumption that there is a $^1S_0$ final-state interaction between two of the neutrons, the other two not interacting. We find, too, that deuteron production is down by a factor of $\approx 10^3$ from proton production, and that the proton spectrum indicates a stronger-than-expected interaction between the three neutrons in the final state. Lower limits for the production of a tri- or tetraneutron are set.

I. INTRODUCTION

THE n-n interaction at low energies has been extensively studied through reactions such as $D(n,p)2n$,[1] $^3H(n,d)2n$,[2] and $T(d,^3He)2n$,[3] and through a different approach by the reaction $\pi^-D \rightarrow 2n\gamma$,[4] where in the final state only the two neutrons are strongly interacting. The theory for the analysis of the data obtained in these experiments is well enough known[3,5–7] that it is not discussed here.

On the other hand, data on the three- and four-neutron systems are scarce and inadequate, and theoretical predictions are contradicting and inconclusive.

A. Three-Neutron System

The ^3n has been searched for through the reaction $^3H(n,p)3n$. In 1965 Ajdacic *et al.* reported observing a proton distribution of energy that led to a ^3n bound by about 1 MeV.[8] This experiment was repeated later at Oak Ridge National Laboratory,[9] and no evidence for the existence of the ^3n system was observed.

A paper by Mitra and Bhasin[10] predicts the existence of the ^3n. They argue that only a moderate ^3P attractive force is needed between all neutron pairs to yield a bound ^3n system, and they predict an $(LSJ)=(1,\frac{3}{2},\frac{1}{2})$ state as the most likely, with $(1,\frac{3}{2},\frac{3}{2})$ a second best. Mitra and Bhasin comment that the existence of the ^3n is independent of the ^4n, for in the latter the $^1S_0$ re-

[1] K. Ilakovac, L. G. Kuo, M. Petravic, and I. Slaus, Phys. Rev. **124**, 1923 (1961).
[2] V. Ajdačić, M. Cerineo, B. Lalović, G. Paić, I. Šlaus, and P. Tomaš, Phys. Rev. Letters **14**, 442 (1965).
[3] E. Baumgartner, H. E. Conzett, E. Shield, and R. J. Slobodrian, Phys. Rev. Letters **16**, 105 (1966).
[4] R. P. Haddock, R. Salter, M. Zeller, J. B. Czirr, D. R. Nygren, and Tin Maung, Phys. Rev. Letters **14**, 318 (1965).
[5] Kirk W. McVoy, Phys. Rev. **121**, 1401 (1961).
[6] K. M. Watson and R. N. Stuart, Phys. Rev. **82**, 738 (1951).
[7] D. Y. Wong and H. P. Noyes, Phys. Rev. **126**, 1866 (1962).
[8] V. Ajdacic, M. Cerineo, B. Lalovic, G. Paic, I. Slaus, and P. Tomas, Phys. Rev. Letters **14**, 444 (1965).
[9] S. T. Thornton, J. K. Blair, C. M. Jones, and H. B. Willard, Phys. Rev. Letters **17**, 701 (1966).
[10] A. N. Mitra and V. S. Bhasin, Phys. Rev. Letters **12**, 523 (1966).

pulsive interaction plays the bigger role, while such a force is negligible in the ^3n case.

It is worthwhile noting that the rule of Baź, Goldanskii, and Zel'dovich, which states that the binding energy of the (2m+2)th neutron is always greater than the binding energy of the $(2m+1)$th neutron, and which would tie the nonexistence of ^3n with the nonexistence of ^4n, does not necessarily apply to the lightest nuclei, for it is derived from shell-model considerations.

Okamoto and Davies[11] assume a $(1, \frac{3}{2}, \frac{1}{2})$ state, too, but obtain a ^3n state unbound by about 10 MeV. They use potentials with parameters consistent with the known ^{3}H and ^{3}He data. They point out that light neutron nuclei should also be unbound according to the systematics of nuclei with $n=3$ and $n=2$.

Phillips, using the Faddeev equations and what is known of the two-nucleon interactions,[12] arrives at an unbound ^3n. All the authors referred to make the drastic assumption that the interactions in the three-nucleon systems are due to a combination of pair interactions. As pointed out by Noyes,[13] these approaches are not far enough along to show if experimental data can be interpreted purely in this way or if actual three-body forces exist.

B. Four-Neutron System

The ^4n has been searched for by looking for its signature in breakup of medium-weight nuclei,[14] or breakup of light nuclei such as π^- ^{7}Li $\rightarrow$ ^4n ^{3}He.[15,16] (In this same experiment detection of the reaction π^- ^{7}Li $\rightarrow$ ^{3}H ^{4}H,[15] with $T=1$ or $T=2$ for the ^4H, was also reported.)

Another approach has been to observe the effects of interactions of the four neutrons on the phase space of one observed particle. Such an experiment can shed light not only on the existence of a bound state, but also on the actual interactions between the neutrons.

The reaction studied was π^- ^{4}He $\rightarrow$ π^+ $4n$.[17,18] No ^4n was found, and the CERN group[18] that performed this experiment finds a phase space for the π^+ that can be explained by a final-state interaction between *two neutrons only*. The resolution in this experiment was an order of magnitude larger than the expected binding energy of the ^4n, and therefore the results are not conclusive.

Tang and Bayman predict that two dineutron clusters will not be bound, and further that the relative energy of the dineutron clusters goes down monotonically as a function of increasing radius.[19] This would lead one to believe that no ^4n resonance exists either. They use for their calculation the n-n singlet-even potential and a triplet-odd potential assumed to be zero except for a hard core of small radius. These authors point out that inclusion of a weak attractive potential in the triplet-odd state does not change their conclusion.

The question of the ^4n is tied directly with excited states of ^{4}He, and a review of this field is of consequence.

C. Excited States of ^{4}He

The literature abounds with experimental data and theoretical analysis on the ^{4}He nucleus.[20–29] An adequate review is afforded by Argan *et al.*[29] They summarize what is known about the problem as follows. One can believe any of the following:

1. (a) The triplet ^{4}H-^{4}He*-^{4}Li exists,[15,30,31] with $E\approx 24$ MeV and $T=1$.

(b) The reported levels at 21 and 22 MeV are the same, with $T=0$. (They could represent the $P_{3/2}$-$P_{1/2}$ spin-orbit splitting, but then a $T=1$ value would be expected as above. For such a T value excited states of ^{4}Li and ^{4}H should exist at ≈ 22 MeV. Experimentally they have not been seen.)

(c) There exists a $T=2$ state at 30 MeV.

(d) The 20-MeV level exists and has $T=0$ or indefinite isospin.

2. The 20-, 24-, and 30-MeV levels are "quasistates,"[32] the only "true" level being the one at 22 MeV with $T=0$; there should exist a second "true" state at ≈ 24 MeV and $T=1$. They conclude with the observation that present knowledge of the nuclear structure of ^{4}He is scanty and sometimes contradictory.

---

[11] K. Okamoto and B. Davies, The University of New South Wales Report (unpublished).
[12] A. C. Phillips, University of Sussex Report (unpublished).
[13] H. Pierre Noyes, Stanford University Report No. SLAC-PUB-256, 1967 (unpublished).
[14] O. D. Brill, N. I. Venikov, A. A. Kuraschov, A. A. Ogloblin, V. M. Pankratov, and V. P. Rudakov, Phys. Letters **12**, 51 (1964).
[15] R. C. Cohen, A. D. Kanaris, S. Margulies, and J. L. Rosen, Phys. Letters **14**, 242 (1965).
[16] R. C. Cohen, A. D. Kanaris, S. Margulies, and J. L. Rosen, Phys. Letters **16**, 292 (1965).
[17] R. E. P. Davis, A. Beretvas, N. E. Booth, C. Dolnick, R. J. Esterling, R. E. Hill, M. Raymond, and D. Sherden, Bull. Am. Phys. Soc. **9**, 627 (1964).
[18] L. Gilly, M. Jean, R. Neunier, M. Spighel, J. P. Stroot, and P. Duteil. Phys. Letters **19**, 335 (1965).
[19] Y. C. Tang and B. F. Bayman, Phys. Rev. Letters **15**, 165 (1965).
[20] Y. C. Tang, Bull. Am. Phys. Soc. **11**, 9 (1966).
[21] G. Charpak, G. Gregoire, L. Massonnet, J. Saudinos, J. Favier, M. Gusakow, and M. Jean, Phys. Letters **16**, 54 (1965).
[22] Carl Werntz, Phys. Rev. **133**, B19 (1964).
[23] D. U. L. Yu and W. E. Meyerhof, Stanford University Institute of Theoretical Physics Report No. ITP-189, 1965 (unpublished).
[24] W. E. Meyerhof and J. N. McElearney, Nucl. Phys. **74**, 533 (1965).
[25] R. Frosch, R. E. Rand, M. R. Yearian, H. L. Crannell, and L. R. Suelzle, Phys. Letters **19**, 155 (1965).
[26] W. E. Meyerhof, Rev. Mod. Phys. **37**, 512 (1965).
[27] A. de Shalit and J. D. Walecka, Stanford University Report No. ITP-193 and SLAC-Pub.-160, 1965 (unpublished).
[28] N. A. Vlasov and L. N. Samoilov, At. Energ. (USSR) **17**, 3 (1964) (UCRL-Trans.-1183).
[29] P. E. Argan, G. C. Mantovani, P. Marazzini, A. Piazzoli, and D. Scannicchio, Nuovo Cimento Suppl. **3**, 245 (1965).
[30] T. A. Tombrello, C. Miller-Jones, G. C. Phyllips, and J. L. Weil, Nucl. Phys. **39**, 541 (1962).
[31] M. J. Beniston, B. Krishnamurthy, R. Levi-Setti, and M. Raymond, Phys. Rev. Letters **13**, 553 (1964).
[32] M. S. Kozodaev, R. M. Suliaev, A. I. Filipovv, and I. U. A. Scherbakov, Zh. Eksperim i Teor. Fiz. **33**, 1047 (1957) [English transl.: Soviet Phys.—JETP **6**, 806 (1958)].

A more recent review of the problem is afforded by Meyerhoff and Tombrello.[33] They conclude that a series of levels exists in ^{4}He at excitation energies between 20.2 and 28.5 MeV, even though they mention that there are indications of the existence of a level "around 30 MeV."

II. EXPERIMENTAL METHOD AND APPARATUS

A. Introduction

We decided that the interaction of negative pions with ^{4}He nuclei, if studied at high resolution, could yield valuable information about the problems presented above.

Of the many reactions produced by the π^- at energies lower than those necessary for the production of a second π, we decided to study the channels

$$\pi^-+{}^4\mathrm{He}^*, \quad (1)$$

$$p+3n, \quad (2)$$

$$d+2n, \quad (3)$$

and the double charge-exchange reaction

$$\pi^++4n. \quad (4)$$

In all these channels one particle in the final state is charged, and this affords an easy measurement of its momentum. The reactions mentioned are of interest because: (1) it can yield excited states of ^{4}He with $T=0$, 1, and 2; (2) the high-momentum end of the proton spectrum will reflect the final-state interactions of the neutrons with low relative energy; (3) the deuteron spectrum is distorted by n-n interactions; (4) the phase-space distribution of the π^+ yields information on the final-state interactions of the four neutrons. The π^+-N interaction cross section is much smaller than the n-n cross section and does not affect the π^+ spectrum in an appreciable way.

We expect that the peaks produced by the channel (1) will be readily identifiable from the smooth background produced by inelastic scattering of the π^- in which the final state contains more than two particles (i.e., ^{4}He breakup). These breakup reactions, together with charge exchange, will produce low-energy protons and deuterons, the thresholds for these reactions being lower than the ones from (2) and (3) by about a pion's rest mass.

Since we are not interested in the low-energy end of the proton or deuteron spectra, these backgrounds can be discriminated against by kinematic considerations.

The π^0's produced in charge exchange reactions yield e^+'s through Dalitz decay. We studied this source of background by a Monte Carlo method and decided that the positron acceptance of our spectrometer was negligible in the region of interest, and no π^+-e^+ discrimination was necessary.

B. Experimental Layout

A (242±0.50)-MeV/c π^- beam was focused on a liquid- ^{4}He target, and the products of the reactions were momentum-analyzed at 20° in the laboratory system (lab) by a magnetic spectrometer, to be described later.

This particular beam energy was chosen because it allowed simultaneous analysis of the π^+, p, and D spectra at 20° when the maximum field attainable in our magnet was used (therefore, at maximum attainable resolution). The target exit angle of 20° was chosen for experimental convenience.

C. Beam

The pion beam was produced when the circulating 735-MeV proton beam of the 184-in. Berkeley cyclotron was allowed to strike an internal Be target. It was first bent through 90° in the cyclotron's own field and then another 90° in an external magnet. This large bend provided high momentum separation at the target, which consisted of a 9×2×2-in. liquid-He flask, the long axis being parallel to the beam direction.

The beam was monitored by two sets of counters (see Fig. 1). A_1, A_2, A_3, and A_4 were four $6\times1.5\times\frac{1}{32}$-in. counters overlapped in pairs (A_1 and A_2, A_3 and A_4) so as to yield $\frac{3}{4}$-in. horizontal resolution. B_1, B_2, and B_3 were $2\times0.5\times\frac{1}{32}$ in. and were overlapped so that they covered a 2×1-in. area, with $\frac{1}{4}$-in. horizontal resolution.

Scattering was minimized along the beam line by a combination of He gas bags and vacuum pipes. An integral range curve of the beam was taken by the use of Cu absorbers, and it was found that it consisted of 58±10% π^-'s, 28% μ^-'s, and 14% e^-'s.

For a fine determination of the beam spectrum a thin ($\frac{3}{16}$-in.) carbon target was positioned at 45° to the beam,

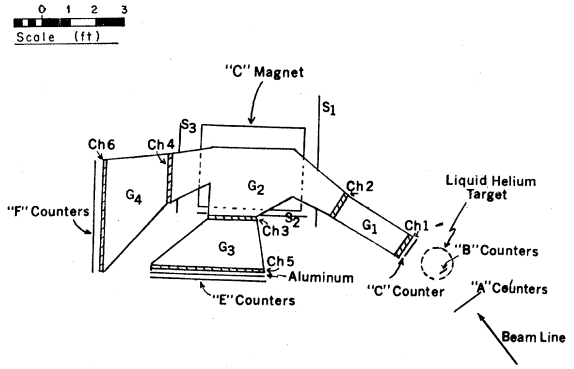

FIG. 1. Spectrometer layout. Pions were detected at the E side, where the aluminum stopped low-energy protons. Protons and deuterons were detected at the F side of the spectrometer. Scattering was minimized by the use of helium-filled gas bags (G_1, G_2, G_3, and G_4); and iron shields (S_1, S_2, and S_3) were attached to the magnet to reduce its stray field.

[33] W. E. Myerhoff and T. A. Tombrello, Nucl. Phys. (to be published).

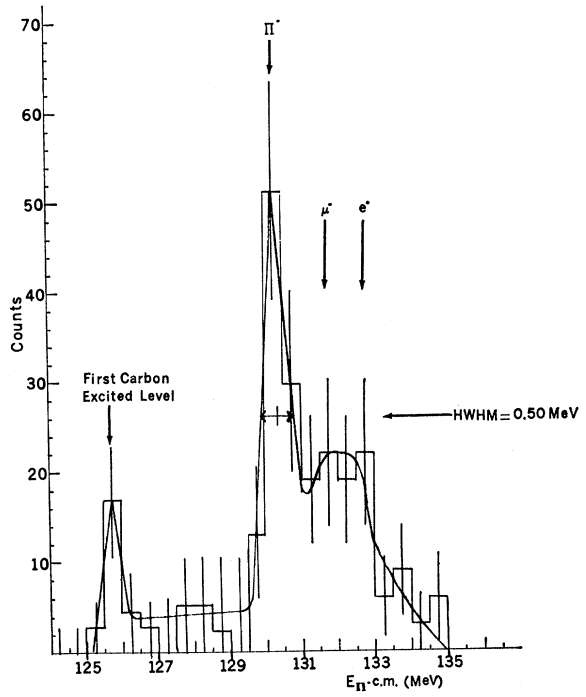

FIG. 2. $\pi^- + C$ elastic scattering spectrum. The arrows indicate where pions, muons, and electrons were expected from kinematic considerations. Muons and electrons could not be differentiated from pions other than by kinematics.

and the elastically scattered negative pions were momentum-analyzed by the spectrometer. The total spread observed was ± 0.50-MeV/c half-width at half-maximum (HWHM) at 237 MeV/c. (No correction was made for energy loss in the target.) This allowed us also to check the calibration by detecting at the same time the first excited level of ^{12}C at 4.4 MeV, as seen in Fig. 2.

D. Spectrometer

Figure 1 shows the spectrometer layout. If the magnetic field, an entrance line, and an exit point are known in a particle's trajectory, the momentum of that particle is uniquely determined. If a second point on the exit path is known, the problem is overdetermined, and consistency can be checked for.

The field was produced by a 16×36-in. "C" magnet with an 8-in. gap. A 2-in.-thick (S_1) iron shield with an 8-in. gap was provided to assure that no bending occurred in the particle's incoming path, and two $\frac{5}{8}$-in. shields with 22×18-in. holes were added on the exit sides to reduce the extent of the magnet's stray field (S_2 and S_3).

The coordinates of the incoming track were determined by two 8×8-in. magnetostrictive readout spark chambers (chambers 1 and 2). By each side of the magnet we placed a 22×18-in. spark chamber (chamber 3 or 4) followed by a 49×17-in. chamber (chamber 5 or 6). Counter C was $\frac{1}{32}$ in. thick by 4 in. wide by $2\frac{5}{8}$ in. high on the side farthest from the pion beam line and $2\frac{3}{8}$ in. high on the side closest to it. The E and F counters were 25×18×0.25 in.

Helium gas bags (G_1, G_2, G_3, and G_4) connected the chambers to minimize particle scattering.

Low-momentum protons and deuterons and all pions went through the "E" side of the spectrometer. The heavy particles did not reach the E counters because an aluminum slab placed between chamber 5 and these counters acted as a filter, completely stopping the protons or deuterons, but having practically no effect on the pions.

The heavy particles in the momentum range of interest went through the F side of the setup, and the time of flight between the C counter and either F_1 or F_2 was recorded onto tape.

The time-of-flight data were used to calculate the masses of the particles from knowledge of the momentum and distance traveled. Given that we were seeking to separate particles whose masses went as M_p, $\approx 2M_p$, $\approx 3M_p$, no great accuracy in time resolution was necessary for the energy range we worked in. Other data stored consisted of a flag for each of the A, B, E, or F counters that produced the trigger.

For chambers 1, 2, 3, and 5 to be fired, the logic requirement was

$$[(A_1 \text{ or } A_2 \text{ or } A_3 \text{ or } A_4)(B_1 \text{ or } B_2 \text{ or } B_3)(C)] \times[(E_1 \text{ or } E_2)(E_3 \text{ or } E_4)];$$

similarly, for chambers 1, 2, 4, and 6 to fire we required

$$[(A_1 \text{ or } A_2 \text{ or } A_3 \text{ or } A_4)(B_1 \text{ or } B_2 \text{ or } B_3)(C)] \times[(F_1 \text{ or } F_2)(F_3 \text{ or } F_4)].$$

We ran with the spectrometer in one of two modes: (i) π^-, where only ABCE coincidences were accepted, and the data on π^--He elastic and inelastic scattering were taken; and (ii) π^+, where both ABCE and ABCF coincidences were accepted, and both the π^+ spectra and protons and deuterons were observed.

Runs were effected for each spectrometer mode both with the target full and empty, to obtain the background sections from the target assembly. In most cases the background was negligible, since the good spatial resolution of the wire chambers allowed us to define a region smaller than the flask and thus discriminate against particles coming from the walls of the flask or other parts of the target assembly.

The spark chambers consisted of four planes of wires: two high-voltage (HV) central planes and two grounded outside ones. Each HV-ground pair was fired by a different capacitor. This decoupled each gap so that we effectively had two spark chambers in each assembly, with only the 90% Ne-10% He gas mixture flowin through the chamber in common. A small amount of ethyl alcohol was added to the gas to act as a spark

quencher, and a 35-V clearing field was used to reduce the sensitive time of the chambers.[34]

Data were collected by the magnetostrictive-readout method[35–38] onto magnetic tape. A novel feature was the use of delay lines to reduce the number of scalers needed. These storage devices are discussed in Ref. 39. Signals from the magnetostrictive lines were differentiated, zero crossed, and then timed by 20-MHz scalers (Fig. 3.). The output of each plane in the chambers consisted of a number for the spark position and another for the total length or "fiducial" distance.

Details on the construction and performance of these chambers can be found in the thesis by one of the authors (L. K.).[40] We summarize our findings here as follows:

a. Accuracy. Track location accuracy was tested prior to the experiment by use of cosmic rays, and later by use of experimental data. We find that, using 20-MHz scalers and and a wire separation of 1.04 mm, we can locate the position of the spark to within 0.33 mm. A typical distribution of the difference between the track location by a plane in the chamber and the actual track is seen in Fig. 4.

b. Efficiency. Before running we checked chamber efficiency as a function of voltage, and found that optimum running conditions were achieved at approximately 10 kV.

Two efficiencies can be considered here:

(*i*) *Efficiency per plane:* For this case we say that a wire plane is 100% efficient if it contributes a coordinate for every event. Once the voltage, clearing field, gas

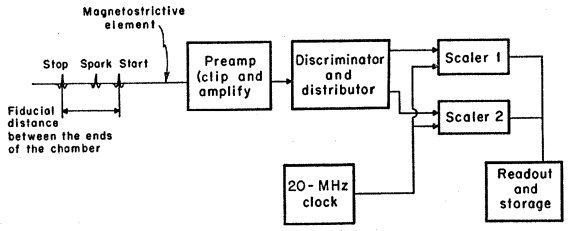

FIG. 3. Simplified logic for magnetostrictive signal processing. The first signal starts both scalers, the second and third signals turn scalers 1 and 2 off, respectively.

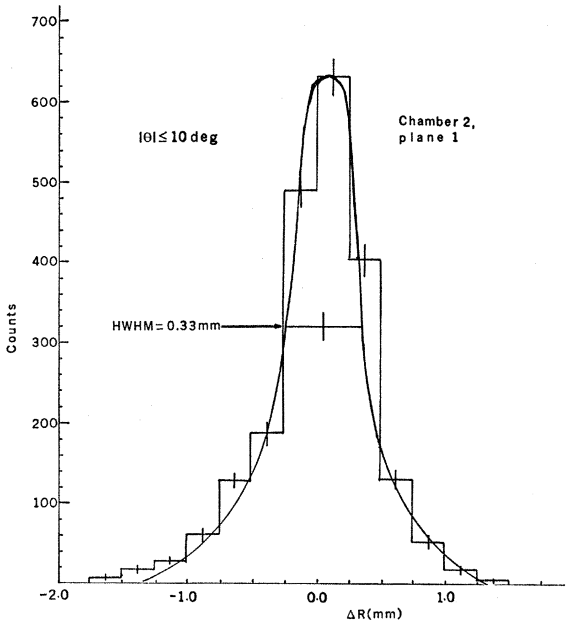

FIG. 4. Deviation ΔR between the coordinate as given by a single plane and a previously determined line. All but one plane of two spark chambers were used to determine the line from which the deviation of the coordinate of the remaining plane was measured. The tails of the distribution reflect the well-known [J. G. Rutherglen and J. M. Paterson, Rev. Sci. Instr. 32, 522 (1961)] tail in the correlation of sparks to tracks.

mixture, and triggering delay were fixed (as they must be during running), we checked plane efficiency as a function of angle for cases in which no more than two sparks occurred. The results are presented in Table I.

(*ii*) *Chamber efficiency:* The data produced by the chambers will still be useful even though not every plane has contributed a coordinate. It is of interest to know the percentage of four-plane, three-plane, and two-plane fits that were present, because even though a two-plane fit is enough to determine a point, if we want to resolve the location of two or more sparks we need at least three coordinates. Then we define as 100% efficient a chamber where *all* events are determined by three- or four-plane fits. The data were taken, as in (*i*), for cases in which no more than two sparks were present, and are summarized in Table II.

III. DATA ANALYSIS

A. General Analysis

We describe now the program used for analysis of the data. The number of counts between the first and last wires in a chamber plane (fiducial counts) were con-

TABLE I. Average plane efficiency.

Chamber	$\|\theta\|<10°$	$\|\theta\|\leqslant 20°$	$20°\leqslant\theta\leqslant 40°$
Front	98.9%	...	...
Back	...	96.7%	94.8%

[34] W. A. Wenzel, University of California, Lawrence Radiation Laboratory Report No. UCRL-11319, 1964 (unpublished).
[35] V. Perez-Mendez and J. M. Pfab, Nucl. Instr. Methods 33, 141 (1965).
[36] V. Perez-Mendez and J. M. Pfab, University of California Lawrence Radiation Laboratory Report No. UCRL-11620, 1964 (unpublished).
[37] F. A. Kirsten, V. Perez-Mendez, and J. M. Pfab, University of California, Lawrence Radiation Laboratory Report No. UCID-2629, 1965 (unpublished).
[38] Victor Perez-Mendez, Proceedings of the 1966 International Conference on Instrumentation for High Energy Physics, Stanford, 1966 (unpublished).
[39] F. A. Kirsten, K. L. Lee, and J. Conragan, IEEE Trans. Nucl. Sci 3, 583 (1966); V. Perez-Mendez, R. L. Grove, and K. Lee, University of California Lawrence Radiation Laboratory Report No. UCID-2839, 1967 (unpublished).
[40] L. Kaufman, Ph.D. thesis, University of California Report No. UCRL-17605, 1967 (unpublished).

TABLE II. Average chamber efficiency.

Chamber	Four-plane	Three-plane	Two-plane	Total
Front	93.2%	6.7%	0.1%	99.9%
Back	87.7%	11.6%	0.7%	99.3%

tinuously updated. As it turned out, this number did not vary by more than one count. The counts produced by sparks were then normalized by the fiducial distance, and a generalized least-squares routine was used to determine the x, y coordinates of the sparks in the chambers. This coordinate was given as a projection on the center plane of the chamber, so that the information on the z coordinate of each one of the planes was not used.

The next step consisted of determining all the possible tracks between chambers 1 and 2 and between 3 and 5 (or 4 and 6). The former were checked to see that they came from the target and did not hit the magnet pole piece, and then were matched with the lines in the back chambers. The target check was done by taking the intersection of the lines as given by the front chambers with the plane on which the trajectory of the incoming pion lay, this plane being determined by the A and B counters. Thus we could determine the location of the origin of the event within 0.4 cm. The matching of the entrance and exit lines of the spectrometer was performed by a polynomial fit, this polynomial having been constructed on the basis of a previous knowledge of the orbits through the magnet.

Once the correct combination of points was known, the program constructed new lines between them. This was done by a generalized least-squares fit to the coordinate as given by each plane, thus taking into account the z positions of that plane. Such a line was called "best line."

The best-line coordinates were used together with an integration and iteration routine to determine the particle's momentum. A second integration and iteration yielded values for the momentum that never varied by more than 0.1% from the values obtained in the previous step.

Since just three points and the magnetic field are needed to determine the momentum uniquely, the fourth point measured can be compared with the one predicted by the integration routine.

For this purpose the differences ($\Delta\theta$ in the horizontal and $\Delta\phi$ in the vertical planes) between the measured and predicted angles in the back chambers were determined, and only events within bands 1.5° and 3.5° wide, respectively, were accepted. Figure 5 shows $\Delta\theta$ and its acceptance band. Once the momentum was known, the program determined whether the particle was a pion, proton, or deuteron from time-of-flight information and flags stored on tape, and corrected the momentum for energy loss in spectrometer and target. The energy loss of the incoming pion and scattering angle were computed too, and a transformation to the center-of-mass system was performed.

Finally events were weighted to correct for spectrometer acceptance and π decay in flight, and histogrammed in 0.5- and 1-MeV bins.

B. Error Estimates

The main sources of eror in the determination of the momentum are considered below.

1. Determination of the Point of Intersection in the Target

This is an important parameter, since the program uses it to compute the correct length of liquid He the incoming and outgoing particles traversed, and then, using that distance, corrects for energy loss in the target.

The uncertainty in energy produced by the finite width of the A and B counters (see Secs. II C and III A)

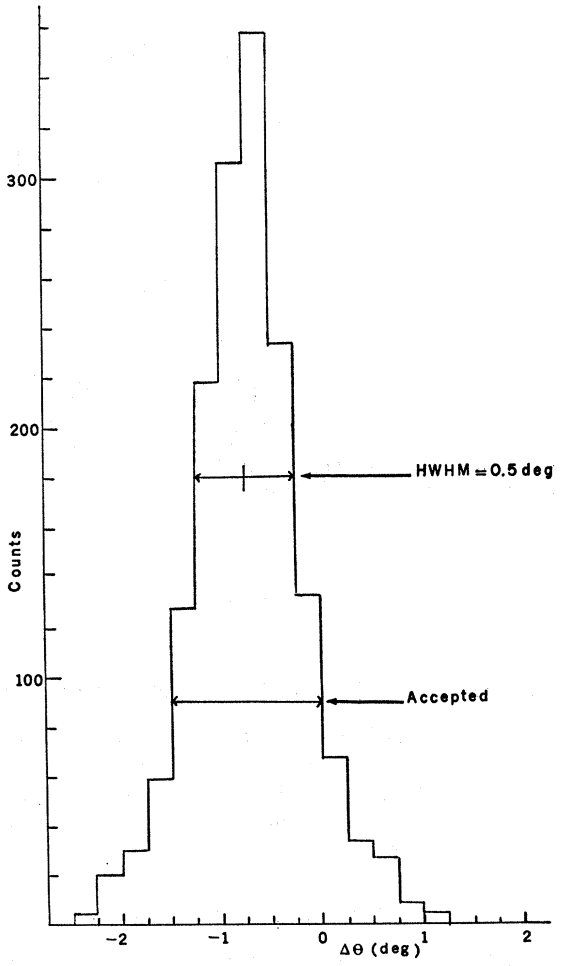

FIG. 5. Angle $\Delta\theta$ between the line measured by chambers 3 and 5, and the line computed from tracks in chambers 1, 2, and 3. The displacement of the center of the distribution is due to a $\frac{1}{32}$-in. displacement of the rig used to map the field. Events were accepted if they fell within the 1.5° band so labeled.

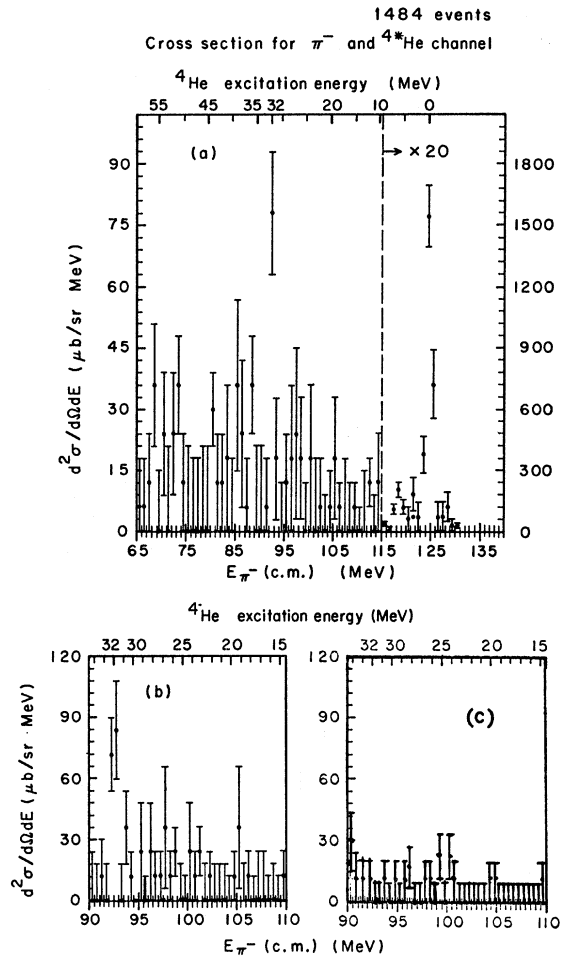

FIG. 6. π^- spectrum in the $\pi^-+{}^4$He* channel. (a) Spectrum with background subtraction and weighting as in text, shown in 1-MeV bins; (b) inelastic-region spectrum, same as in (a), shown in 0.5-MeV bins; (c) weighted background events in the inelastic region, shown in 0.5-MeV bins. The (32±1)-MeV peak is 3.5 standard deviations above the mean inelastic spectrum.

amounts to 0.1, 0.1, and 0.25% for pions, protons, and deuterons in the high-energy ends of their respective spectral distributions.

2. Determination of the Scattering Angle in the Target

The uncertainty in this case is produced by scattering in the liquid He and by finite width of the A and B counters. The total uncertainty expected is $\Delta\theta\approx\pm 2.5°$, which produces momenta uncertainties approximately equal to the ones above.

3. Scattering in the Spectrometer

This factor—and, to a lesser degree, chamber coordinate resolution—produced an uncertainty in the measured angle of entrance into the magnet.

The effects of scattering were studied by approximating the actual field by a uniform rectangular one.

We find that in most cases, including the effects of uncertainties in spark location in the chambers, the values are $\Delta p/p<0.6\%$ for pions, $\Delta p/p<0.2\%$ for protons, and $\Delta p/p<0.6\%$ for deuterons.

4. Energy Resolution

Combining the uncertainties discussed in *1*, *2*, and *3* and including also the momentum spread of the incident beam, we estimate that in the high-energy end of the respective spectra we would have $\Delta E(\pi)\leqslant 1.0$ MeV, $\Delta E(p)\leqslant 0.6$ MeV, and $\Delta E(d)\leqslant 1.2$ MeV.

IV. RESULTS, INTERPRETATION, AND CONCLUSIONS

A. $\pi^-+{}^4$He and $\pi^-+{}^4$He* Channels

Figure 6 shows the scattered π^- energy spectrum in the c.m. system. The cross sections given are corrected for (a) μ^- and e^- contamination of the initial beam, (b) solid-angle acceptance of the helium target, (c) spectrometer acceptance, and (d) π decay in flight. The background has been subtracted, and can be seen in Fig. 6.

Our resolution is determined by the full width at half-maximum (FWHM) (≈1 MeV) of the elastic peak.

The study of this reaction shows one inelastic peak located at 32±1 MeV relative to the elastic scattering peak as shown in Fig. 6. This peak is 3.5 standard deviations above the mean inelastic spectrum, and is narrower than our experimental resolution. This level can have a T spin of 0, 1, or 2. In a previous experiment Charpak *et al.*[21] discovered a 30-MeV level formed in the reaction $\pi^++{}^6\text{Li}\rightarrow 2p+{}^4\text{He}^*$. This level is quite wide and overlaps ours, and although the authors considered it as a manifestation of peripheral reactions, Tang[41] in a subsequent paper argues for the existence of a $T=0$ level at ≈30 MeV. Measday and Palmieri[42] present arguments for the existence of a $T=1$ contribution to the level at that energy.

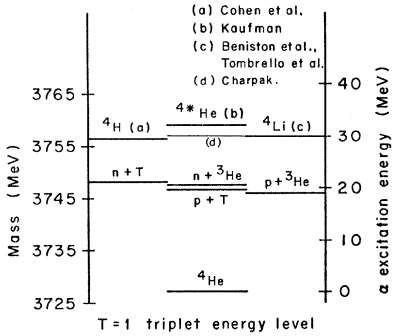

FIG. 7. Some observed levels and thresholds for the $A=4$ system.

[41] Y. C. Tang, Phys. Letters **20**, 299 (1966).
[42] D. F. Measday and D. N. Palmieri, Harvard University Report, 1967 (unpublished).

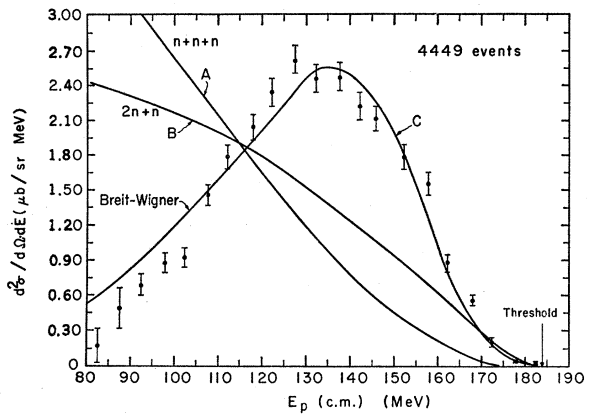

FIG. 8. Proton spectrum in the $p+3n$ channel weighted as in text, shown in 5-MeV bins. (A) Phase space. (B) Phase space distorted by the $^1S_0$ interaction between two neutrons. (C) Breit-Wigner fit for a 3-n system unbound by 15 MeV, and a width $=65\times10^{-8}k^3$ (k in MeV). All curves are normalized to the area of the observed spectrum in the energy range shown.

There is evidence[15] that ^{4}H unstable against dissociation exists, even though particle-stable ^{4}H has not been seen. As we mentioned before, Cohen *et al.* observed the reactions ^{6}Li(π^-,d)^{4}H and ^{7}Li(π^-,t)^{4}H, finding ^{4}H with $0<$B.E.<5 MeV against its breakup into four free nucleons.

There is evidence for the existence of ^{4}Li* as reported by Tombrello *et al.*[30,33]; furthermore, Beniston *et al.*[31] observe that analysis of the π^- and p momenta in the decay of the ^{4}He$_\Lambda$ hyperfragment (^{4}He$_\Lambda\rightarrow\pi^-p^3$He) yields evidence of a ^{4}Li state with an energy that corresponds to $\approx$30-MeV excitation of the α particle. Even though Beniston's data are questioned at this time, the existence of this level seems to be well determined.[33] Our negative results in the π^++$4n$ channel tend to indicate that ^4n does not exist, therefore we believe that the present data indicate the existence of the isospin triplet, and that it corresponds to an excited level of ^{4}He with $E\approx32$ MeV (Fig. 7).

B. $p+3n$ Channel

Figure 8 shows the proton energy spectrum. Superimposed on it we see the distributions to be expected from phase space (curve A), and the effect of adding the singlet-even interaction between two of the neutrons in the final state (curve B).

Cross sections are corrected for factors (a), (b), and (c) as seen in A. The background was negligible.

Our experimental setup allowed us to search for trineutrons of 0- to 50-MeV binding energy. No events were seen in this region. Since one event would have been equivalent to 2.5×10^{-2} μb/sr, we have set the upper limit for ^3n formation to be this value.

As seen in Fig. 8, the proton spectrum shows a pronounced peaking at 130 MeV. This corresponds to an energy of 53 MeV for the three neutrons in their center of mass. The proton spectrum was not measured below 80 MeV. The reason for this is that from approximately this point down the π^- ^{4}He$\rightarrow p$ $3n$ π^0 channel and ^{4}He breakup reactions contribute, and the spectrum of the proton is no longer uniquely determined by the reaction of interest. This makes the normalization nonunique too. On the other hand, we can reasonably assume that, from the quick drop in cross section observed around 90 MeV, most of the area of the curve concentrates in the region measured.

The comparison of immediate interest is made with respect to phase space and phase space altered by the $^1S_0$ interaction between two of the neutrons in the final state. (The Pauli principle voids the possibility that more neutrons can be in a relative S state.) For this interaction we use standard effective-range theory with a 70-keV scattering length.

The results are shown normalized in two ways. In Fig. 8 we compare the spectra with equal areas in the region where measurements were performed; in Fig. 9 we see the same spectra normalized in such a way that the peaks are at the same height. It is easy to see that the spectra shown differ widely from that observed. We call the reader's attention to the fact that addition of a final-state interaction between the proton and one (or more) of the neutrons will shift the proton spectrum towards the low-energy end, contrary to what is seen.

As a purely phenomenological fit we used a Breit-Wigner–like resonance among the three neutrons, assuming the decay of the p-$3n$ system to go through an $l=1$ channel. This makes the width proportional to the third power of the relative momentum. The results

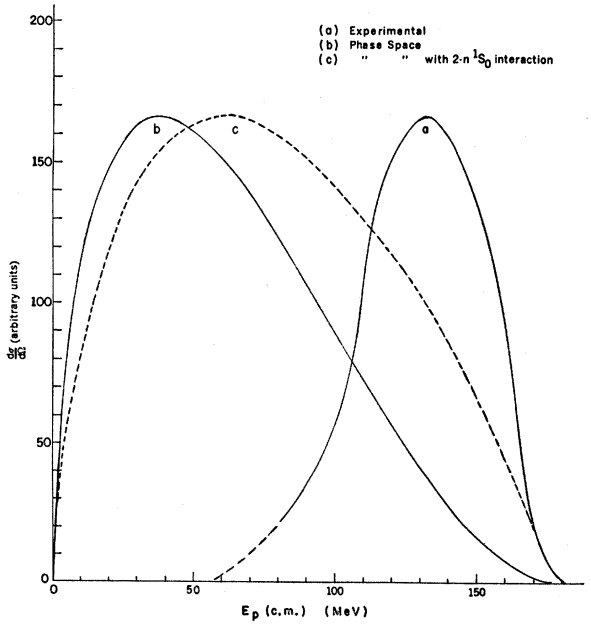

FIG. 9. A comparison of the observed and computed proton spectra in the $p+3n$ channel, shown normalized to equal heights. Curve a shows the observed spectrum, b shows phase space, and c shows the effect of adding the $^1S_0$ interaction between two of the neutrons.

provide a satisfactory fit to the data, and can be seen in Fig. 8, curve C.

A possibility to consider is that we are dealing with a direct-reaction mechanism. In this case, the high-energy protons would arise from π^- absorption by p-p pairs, producing a proton and a neutron which share the energy of the pion, and two other neutrons that are spectators and carry energies of the order of their Fermi momenta in the α nucleus. Were this to be a purely two-body absorption, we would expect the proton to carry about 122 MeV in the c.m. system; this is lower than the observed most probable proton energy of 130 MeV. The width of this peak (caused by the internal energy of the target nucleons) should be approximately 20 MeV, narrower than the observed width. Since this mechanism does not seem to match the data, we should consider the possibility that the observed effects are due to a three-body interaction.

With the data available at present we can give no simple answer. Further experiments providing considerably more data will be needed in order to clarify these points.

C. $d+2n$ Channel

Only four deuterons were seen in the range from 470 MeV/c to threshold at 801 MeV/c in the lab. This yields the result

$$\frac{\sigma_{\pi^-+\mathrm{He}^4\to p+3n}}{\sigma_{\pi^-+\mathrm{He}^4\to d+2n}}=1150\pm 50\%.$$

The cross section for this reaction in the c.m. system is $\sigma=0.0012$ μb/sr MeV $\pm 50\%$. These cross sections are corrected as in Sec. IV B. Background was nonexistent.

The low cross section found for this reaction yields a low probability for the dnp and dd components of the wave function of the α particle. Furthermore, it tends to indicate that the final-state interaction between the proton and one of the neutrons in the $p+3n$ channel is small.

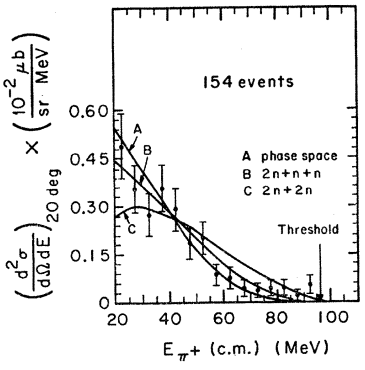

FIG. 10. π^+ spectrum in the π^++4n channel. Spectrum with background subtraction and weighting as in text, shown in 5-MeV bins. Curve A shows phase space, curve B shows the effect of adding the $^1S_0$ interaction between two of the neutrons, and curve C shows the effect of adding the $^1S_0$ interaction between two neutrons in each pair. χ^2 tests yield confidence levels of 32%, 50%, and less than 1%, respectively.

D. π^++4n Channel

The resultant π^+ spectrum is shown in Fig. 10. The experimental resolution was 1 MeV, as in the case of π^-'s. Corrections were made as in Sec. IV A, and background was negligible.

The 1-MeV resolution available in this experiment allowed careful search for a tetraneutron. Our experimental setup allowed us to search in a region of up to 40-MeV ^4n binding energy. Since no events were seen in this region, we set an upper limit of 7×10^{-4} μb/sr on ^4n production, this being the value of the cross section that would have been yielded by one event. Three randomly distributed events were obtained in the region 90 MeV $\leq E_{\pi^+}$(c.m.)$\leq$95 MeV. Superimposed on the observed spectrum can be seen the spectrum predicted by phase space, and the effects of adding the singlet-even interaction between two of the neutrons in one pair ($2n+n+n$), or between the two neutrons in each pair ($2n+2n$). We find that our data fit these calculated spectra with confidence levels of 32%, 50%, and less than 1%, respectively.

Although not inconsistent with phase space, the π^+ energy spectrum is in closer agreement with the findings of Gilly *et al.*[18] Their results indicate two neutrons interacting through a $^1S_0$ potential, the interaction of the other two neutrons not being strong enough to affect the spectrum appreciably. Our method of measurement would not allow us to determine whether the two neutrons in the $^1S_0$ state were produced by double charge exchange or were spectators.

No effects from the three-neutron interaction seen in Sec. IV B manifest themselves here. This would follow from the arguments, presented by Mitra and Bhasin,[10] that P forces play the dominant role in the three-neutron system, while the kernel for the $^1S_0$-wave part of the force (which predominantes in the two- and four-neutron case) is repulsive.[9,10]

ACKNOWLEDGMENTS

The authors are grateful to Professor Burton J. Moyer and Professor A. Carl Helmholz for their support of this work. We are also greatly indebted to many people for the successful completion of this experiment: to Anthony J. Schaeffer for his work in the construction of our data-reducing programs; to Brownlee Gauld and Stephen Williams for their help in setting up and running this experiment, and to Arthur Greenberg for his help with the design of the beam; to Jimmy Vale and the 184-in. cyclotron crew, and to Lou Sylvia and the Accelerator Technician crews, for their cooperation. We wish to thank Dr. Tom Mongan for his work and helpful comments on the analysis of the three-nucleon data.